Biochimica et Biophysica Acta 939 (1988) 124–130
Elsevier

BBA 73912

Effect of fluorophore linkage position of *n*-(9-anthroyloxy) fatty acids on probe distribution between coexisting gel and fluid phospholipid phases

Ning-na Huang [a], Kathryn Florine-Casteel [a,*], Gerald W. Feigenson [a] and Charles Spink [b]

[a] *Section of Biochemistry, Molecular and Cell Biology, Clark Hall, Cornell University, Ithaca, NY and* [b] *Department of Chemistry, SUNY Cortland, Cortland, NY (U.S.A.)*

(Received 31 August 1987)

Key words: Fluorescence quenching; Phospholipid vesicle; Phase separation; Anthroyloxy fatty acid; Fluorescent probe

The quenching of probe fluorescence by spin-labeled phospholipid has been used to determine the distribution of a series of *n*-(9-anthroyloxy) fatty acids between coexisting gel and fluid liquid-crystal phases in multilamellar phospholipid vesicles. The phase distribution ratio in every case is found to favor the fluid lipid phase, but is much greater between fluid and Ca^{2+}-induced gel than between fluid and thermal gel. For a given gel type, *n*-(9-anthroyloxy)stearic acids with $n = 3$, 6, 9 or 12 as well as 11-(9-anthroyloxy)undecanoic acid all exhibit similar behavior, favoring the fluid phase by about a factor of 4 over thermally-induced lipid gel phase and by 18 over Ca^{2+}-induced gel phase. 16-(9-Anthroyloxy)palmitic acid, with the bulky probe at the terminus of the 16-carbon chain, favors the fluid phase less strongly, by a factor of 1.5 or 11 over thermally-induced or Ca^{2+}-induced gel phase, respectively, indicating better packing of this probe in phospholipid gel phases.

Introduction

Fluorescent-labeled probe molecules have proven useful for studying lipid phase behavior. Coexisting solid- and fluid-phase lipid domains have been observed in supported lipid monolayers using fluorescent probes and epifluorescence microscopy [1,2]. Lipid phase separation has been extensively investigated in model phospholipid bilayers, also by use of fluorescent probe molecules [3–7]. Evidence suggesting the existence of lipid domains in biological membranes [8,9] makes even more relevant the understanding of the lipid phase distribution behavior of fluorescent membrane probes.

We have utilized a series of *n*-(9-anthroyloxy) fatty acid probes incorporated into multilamellar

* Present address: Laboratories for Cell Biology, Department of Anatomy, School of Medicine, University of North Carolina at Chapel Hill, Chapel Hill, NC 27514, U.S.A.

Abbreviations: DSC, differential scanning calorimetry; DPPC, 1,2-dipalmitoyl-*sn*-glycero-3-phosphocholine; DSPC, 1,2-distearoyl-*sn*-glycero-3-phosphocholine; DLPC, 1,2-dilauroyl-*sn*-glycero-3-phosphocholine; DOPS, 1,2-dioleoyl-*sn*-glycero-3-phosphoserine; (7,6)-palmitic acid, 2-(6-carboxyhexyl)-2-octyl-4,4-dimethyloxazolidinyl-3-oxy; (7,6)PC, 1-acyl-2-[(7,6)-palmitoyl]-*sn*-glycero-3-phosphocholine; 3-, 6-, 9-, and 12-AS, 3-, 6-, 9-, and 12-(9-anthroyloxy)stearic acid, respectively; 16-AP, 16-(9-anthroyloxy)palmitic acid; 11-AU, 11-(9-anthroyloxy)undecanoic acid; DPH, 1,6-diphenyl-1,3,5-hexatriene; Pipes, piperazine-*N*,*N*′-bis(2-ethanesulfonic acid); $R_{LC/G}$, ratio of fluorophore concentration in the fluid liquid-crystal phase to that in the gel phase.

Correspondence: G.W. Feigenson, Section of Biochemistry, Molecular and Cell Biology, Clark Hall, Cornell University, Ithaca, NY 14853, U.S.A.

phospholipid vesicles in which gel and fluid lipid phases coexist, to examine the effect of the position of attachment of the fluorescent moiety on probe distribution between the two phases. The *n*-(9-anthroyloxy) series was chosen because the fluorescence properties as well as the location of these hydrocarbon probes in single-component phospholipid bilayers have been well characterized [10,11]. In addition, the fact that the 9-anthroyloxy moiety is non-polar reduces the likelihood of its moving to the polar/hydrocarbon interface, as has been observed for 7-nitrobenz-2-oxa-1,3-diazol-4-yl (NBD)-labeled lipids [12].

Both thermally-induced and Ca^{2+}-induced lipid phase separations have been investigated, using a method developed in this laboratory [13,14] whereby fluorescence quenching of a membrane-bound fluorophore by spin-labeled phosphatidylcholine ((7,6)PC) is used to determine probe distribution between the phases. The binary lipid systems examined are dipalmitoylphosphatidylcholine (DPPC)/(7,6)PC, distearoylphosphatidylcholine (DSPC)/(7,6)PC, and dioleoylphosphatidylserine (DOPS)/(7,6)PC $\pm$ Ca^{2+}. Partial phase diagrams for DPPC/(7,6)PC and DSPC/(7,6)PC were obtained using differential scanning calorimetry (DSC). The lipid phase behavior of DOPS/(7,6)PC in the presence of excess Ca^{2+} has been previously determined [15].

Materials and Methods

DOPS, DPPC, and DSPC were purchased from Avanti Polar Lipids Inc. (Birmingham, AL). (7,6)PC was synthesized by condensation of (7,6)-palmitic acid with egg lyso-PC as described previously [4]. The fluorescent probes 3-, 6-, 9-, 12-(9-anthroyloxy)stearic acid (3-, 6-, 9-, 12-AS), 16-(9-anthroyloxy)palmitic acid (16-AP), and 11-(9-anthroyloxy)undecanoic acid (11-AU) were obtained from Molecular Probes Inc. (Eugene, OR). 1,6-Diphenyl-1,3,5-hexatriene (DPH) was from Aldrich Chemical Co. (Milwaukee, WI). Pipes buffer was puriss grade, from A.G. Fluka (Hauppauge, NY). Water was purified through a Milli-Q system (Millipore Corp., Bedford, MA). Organic solvents were HPLC grade. All other chemicals were reagent grade. Lipid purity was established by thin-layer chromatography of 20–50 μg on Adsorbosil Plus P plates (Applied Science, State College, PA) using chloroform/methanol/concentrated ammonium hydroxide (66:30:6, v/v) and hexane/diethyl ether/acetic acid (80:20:1, v/v) for phospholipids and fluorophores, respectively.

Samples for fluorescence experiments were prepared as follows. Aliquots of stock solutions of fluorophore in ethanol were added to phospholipid in chloroform in 10×75 mm borosilicate culture tubes. The mixtures were dried to a thin film under a stream of N_2 gas, further dried under vacuum in the dark for a minimum of 4 h, then hydrated under argon in buffer containing 20 mM Pipes and 100 mM KCl at pH 7.0. DPPC/(7,6)PC and DSPC/(7,6)PC dispersions were incubated for 30–60 min at 45 °C and 58 °C, respectively, at 100 μM lipid concentration, followed by mild vortex mixing. DOPS/(7,6)PC samples of 1–2 mM lipid concentration were incubated at room temperature and briefly vortexed, then further diluted with buffer alone or else buffer containing $CaCl_2$, to a final concentration of 1 mM lipid with or without 2 mM Ca^{2+}. Ca^{2+} was equilibrated by 15 cycles of freezing at -10 °C and thawing in a water bath, as described previously [15]. Lipid blanks were prepared in the same manner as samples containing fluorophore.

Fluorescence measurements were made with a home-built spectrofluorometer [16] equipped with double monochromators in both excitation and emission optics. The excitation/emission wavelengths used were 385/470 nm, with nominal bandwidths of 2 and 16 nm for excitation and emission, respectively. Sample compartment temperature was 25 °C. DOPS/(7,6)PC vesicles were diluted into acrylic cuvettes of 1 cm^2 cross-section (Sarstedt Inc.) containing the same buffer to a final volume of 1.5 ml and lipid concentration of 100 μM. Because of variable sample transfer efficiency to the cuvettes for samples containing DOPS in excess Ca^{2+}, the lipid concentration in the cuvette was determined by phosphate analysis of aliquots removed from the cuvettes immediately following fluorescence measurements [15]. DPPC/(7,6)PC and DSPC/(7,6)PC samples were not diluted further and were not assayed for phosphate. Lipid blank fluorescence typically increased from 5 to 40% of the sample signal as the mole fraction of (7,6)PC increased from 0.0 to 0.8.

DSC measurements on DPPC/(7,6)PC and DSPC/(7,6)PC dispersions were made with a MicroCal MC-2 scanning calorimeter using a scan rate of 0.66 K/min. Vesicles were prepared from stock chloroform solutions as described above, but with lipid concentrations of 0.5–1.0 mg/ml. Samples were de-aerated, placed in the calorimeter cell, then cooled to the appropriate starting temperature and allowed to equilibrate for about 45 min before initiating the scan. Each sample was scanned two or three times to check reproducibility. The thermal transition data were obtained with a computer data acquisition system, and the onset and completion temperatures determined from integral traces of the transition curves. The onset and completion temperatures were corrected for the natural width of the pure lipid transitions, as suggested by Mabrey and Sturtevant [17]. For the lower mole fractions of DPPC or DSPC in mixtures with (7,6)PC, only the liquidus temperature could be determined because the solidus boundary is below 0 °C.

Results

The distribution of fluorescent probe molecules between coexisting gel and fluid liquid-crystal lipid phases can be found by measuring contact quenching of fluorescence by nitroxide spin-labeled phospholipid [13,14]. The method requires the use of binary mixtures of spin-labeled and unlabeled phospholipid whose phase behavior is known. Probe fluorescence is measured as the mole fraction of spin-labeled phospholipid in the vesicles is varied from 0 to 1, generating fluorescence quenching curves. In the two-phase region, the lipid composition of each phase determines the quantum yield of fluorescence for probe molecules in that phase, and hence the ratio of the fluorophore concentration in the liquid-crystal phase to that in the gel phase, $R_{LC/G}$, can be found from the fluorescence quenching data according to

$$F = F_{LC} + \frac{[G]}{R_{LC/G}(1-[G])+[G]}(F_G - F_{LC}) \qquad (1)$$

where F is the measured or calculated fluorescence intensity, $F_{G(LC)}$ is the fluorescence in a

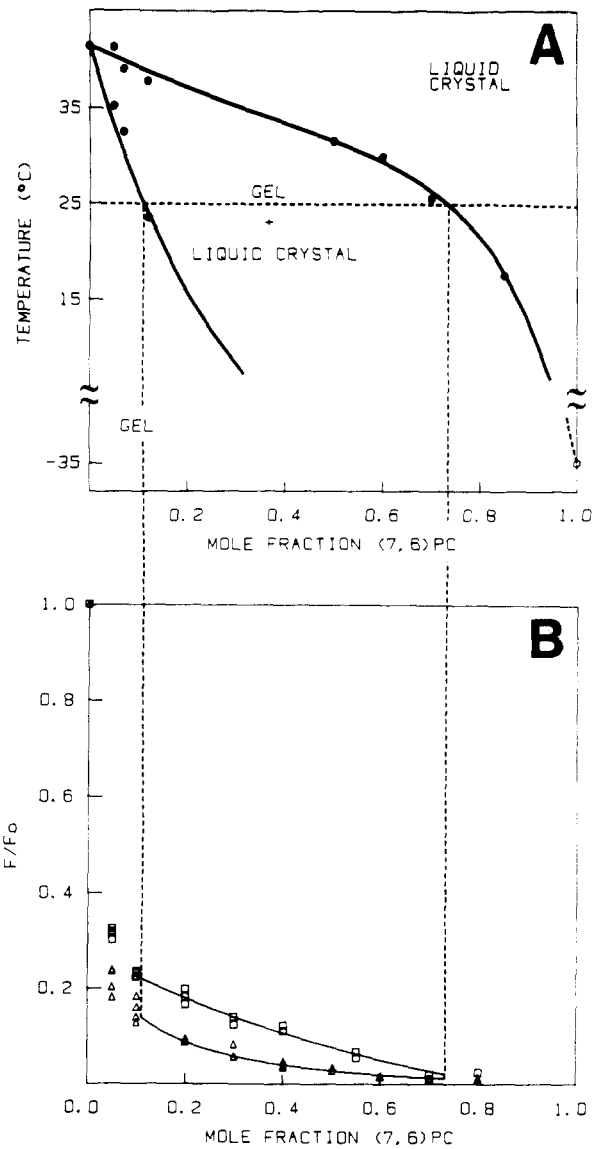

Fig. 1. (A) Partial phase diagram for DPPC/(7,6)PC multilamellar vesicles, illustrating the solidus and liquidus boundaries at 25 °C. Data points were determined by DSC (●) or X-ray diffraction (○). Dashed lines are hypothetical. (B) Fluorescence quenching of 16-AP (□) or 9-AS (△) in DPPC/(7,6)PC multilamellar vesicles at 25 °C. The abscissa is the mole fraction of (7,6)PC in the vesicles and the ordinate is the ratio of fluorescence in the presence (F) and absence (F_0) of (7,6)PC. Probe/lipid molar ratio is 1:1000. Solid lines are theoretical curves calculated according to Eqn. 1 for values of $R_{LC/G}$ of 1.5 (16-AP) and 4.0 (9-AS), using $[(7,6)PC]_G = 0.11$ and $[(7,6)PC]_{LC} = 0.73$.

membrane of the composition at the gel (liquid-crystal) phase boundary, and

$$[G] = ([(7,6)PC]_{LC} - [(7,6)PC])/([(7,6)PC]_{LC} - [(7,6)PC]_G).$$

[(7,6)PC] is the overall mole fraction of (7,6)PC in the vesicles and $[(7,6)PC]_{G(LC)}$ is the mole fraction of (7,6)PC in the gel (liquid-crystal) phase at the boundary of the two-phase region, as determined from the phase diagram. $R_{LC/G}$, the only unknown, is found by fitting the experimental data to theoretical curves of F vs. [(7,6)PC] in the two-phase region calculated from Eqn. 1. Although we describe the probe partitioning in terms of a concentration ratio, recent measurements of its probe concentration and [G]/[LC] independence confirm that it is a true partition coefficient [18]. The most reliable measurements can be made for a lipid mixture for which gel and fluid phases coexist over a relatively large range of vesicle lipid composition at the temperature at which the fluorescence experiment is performed.

Thermally-induced lipid phase separation and probe redistribution were examined in two systems, DPPC/(7,6)PC and DSPC/(7,6)PC at 25 °C. Partial phase diagrams determined by DSC are shown in Figs. 1A and 2A. The gel-fluid lamellar transition range of (7,6)PC of −30 °C to −40 °C was previously determined by X-ray diffraction [15]. In multilamellar vesicles composed of

TABLE I

RATIO OF FLUOROPHORE CONCENTRATION IN THE LIQUID-CRYSTAL PHASE TO THAT IN THE GEL PHASE ($R_{LC/G}$) IN MULTILAMELLAR VESICLES AT 25 °C

Values represent the best theoretical fits to the experimental data, using Eqn. 1. Error indicates the range of $R_{LC/G}$ values which could reasonably fit the data. The larger error for the DSPC/(7,6)PC data results from the combination of steeper fluorescence quenching curves and high lipid blank fluorescence.

Probe	Vesicle composition		
	DPPC/(7,6)PC	DSPC/(7,6)PC	DOPS/(7,6)PC $+Ca^{2+}$
3-AS	2.5±0.5	4 ±1	18±2
6-AS	4 ±1	5 ±3	17±2
9-AS	4 ±1	4 ±2	18±2
12-AS	4 ±1	6 ±3	19±2
11-AU	4 ±1	5 ±2	18±2
16-AP	1.5±0.5	1.5±0.5	11±2
DPH	1.5±0.5	1.5±0.5	12±1 [a]

[a] Previously reported [15].

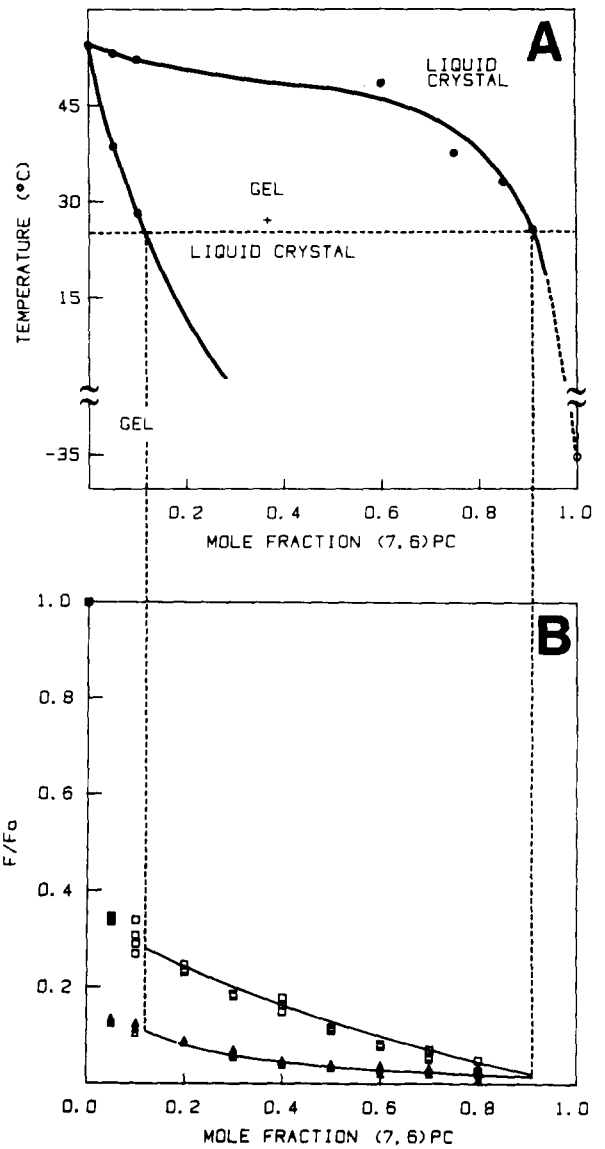

Fig. 2. (A) Partial phase diagram for DSPC/(7,6)PC multilamellar vesicles, illustrating the solidus and liquidus boundaries at 25 °C. Data points were determined by DSC (●) or X-ray diffraction (○). Dashed lines are hypothetical. (B) Fluorescence quenching of 16-AP (□) or 3-AS (△) in DSPC/(7,6)PC multilamellar vesicles at 25 °C. Probe/lipid molar ratio is 1:1000. Solid lines are theoretical curves calculated according to Eqn. 1 for values of $R_{LC/G}$ of 1.5 (16-AP) and 4.0 (3-AS), using $[(7,6)PC]_G = 0.12$ and $[(7,6)PC]_{LC} = 0.91$.

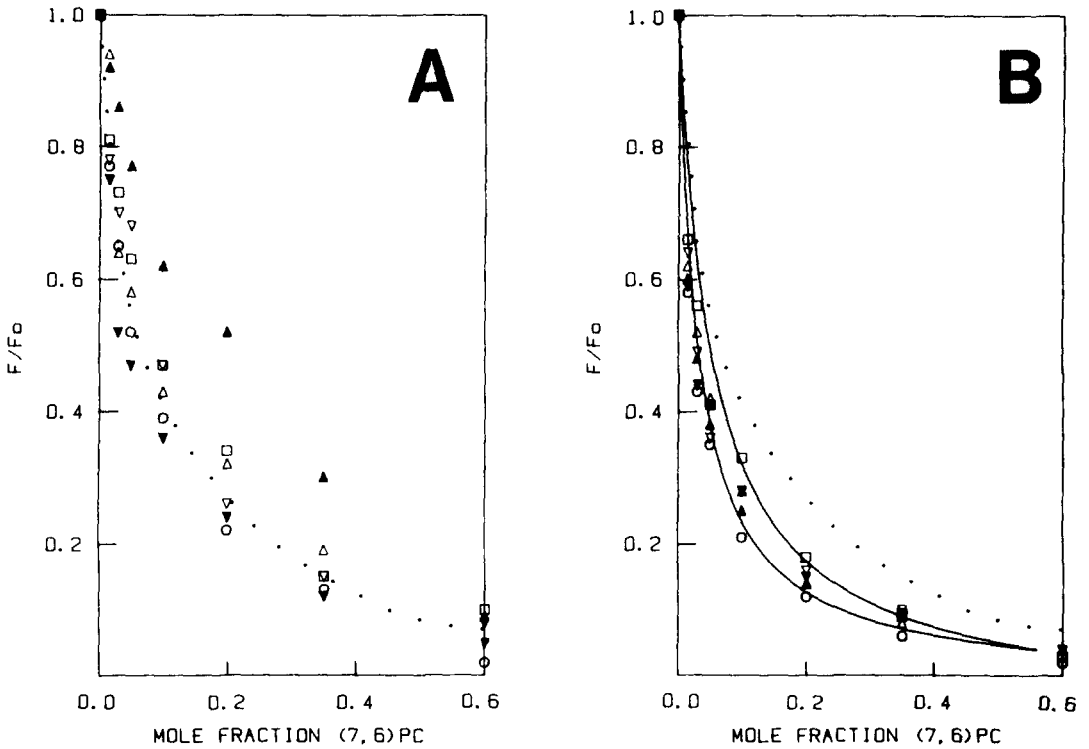

Fig. 3. Fluorescence quenching of 11-AU (▲), 3-AS (△), 6-AS (▽), 9-AS (▼), 12-AS (○), and 16-AP (□) in 100 μM DOPS/(7,6)PC multilamellar vesicles at 25 °C in the absence (A) of presence (B) of 2 mM Ca^{2+}. Data points are averages of triplicate samples of typically 5% fluorescence variation. Probe/lipid molar ratio is 1:1000. The dotted line in (A) represents the average fluorescence quenching of the *n*-AS and 16-AP probes in the absence of Ca^{2+} and is reproduced in (B) for reference. Solid lines in (B) are theoretical curves calculated according to Eqn. 1 for values of $R_{LC/G}$ of 11 and 18, using $[(7,6)PC]_G = 0.00$ and $[(7,6)PC]_{LC} = 0.56$.

DPPC/(7,6)PC, the boundaries of the two-phase region at 25 °C are $[(7,6)PC]_G = 0.11$ and $[(7,6)PC]_{LC} = 0.73$. As Fig. 1B illustrates, the fluorescence quenching data for 16-AP in the phase coexistence region are best fit by $R_{LC/G} = 1.5$. The data for 9-AS, shown in Fig. 1B, as well as that for 6-AS, 12-AS, and 11-AU, are well fit by $R_{LC/G} = 4$, while that for 3-AS is best described by $R_{LC/G} = 2.5$. In DSPC/(7,6)PC vesicles at 25 °C, the phase boundaries are located at $[(7,6)PC]_G = 0.12$ and $[(7,6)PC]_{LC} = 0.91$. The partition behavior of the probes, illustrated in Fig. 2B for 3-AS and 16-AP, is similar to that observed with DPPC/(7,6)PC vesicles, although the considerably higher fluorescence quantum yield of the *n*-AS and 11-AU probes in DSPC compared to DPPC results in steeper quenching curves for these probes.

Ca^{2+} binding to phosphatidylserine in DOPS/(7,6)PC multilamellar vesicles at room temperature results in lipid phase separation into a $Ca(PS)_2$ rigid gel phase and a PC-rich fluid liquid-crystal phase. The boundaries of the two-phase region at $[Ca^{2+}] = 2$ mM are $[(7,6)PC]_G = 0.00$ and $[(7,6)PC]_{LC} = 0.55$–0.60 [15]. As shown in Fig. 3A, all of the *n*-(9-anthroyloxy) probes, with the exception of 11-AU, exhibit similar quenching behavior in fluid-phase DOPS/(7,6)PC. Iodide quenching of 11-AU in egg PC vesicles indicates that this probe is located, at least in part, near the aqueous interface [11]. This location would be consistent with the reduced quenching of 11-AU by (7,6)PC, compared with the other probes shown in Fig. 3A. In the presence of excess Ca^{2+}, all of the probes partition strongly out of the $Ca(PS)_2$ gel phase, as Fig. 3B illustrates. We note that probe fluorescence in pure DOPS multi-

layers was enhanced 5–15% by the addition of Ca^{2+} (data not shown), in agreement with previous observations for the methyl ester of 12-AS [15].

The partition behavior of the *n*-(9-anthroyloxy) fatty acids in the three lipid systems investigated is summarized in Table I. For comparison, results of fluorescence quenching experiments using the well-studied probe 1,6-diphenyl-1,3,5-hexatriene (DPH) are also shown.

Discussion

Using a set of *n*-(9-anthroyloxy) fatty acid membrane probes labeled at different positions along the acyl chain, we have examined how the fluorophore linkage position influences probe packing in phospholipid gel phases and, consequently, probe distribution between coexisting gel and fluid lipid phases. Both thermally-induced and Ca^{2+}-induced gel phases were examined. For a given lipid system, when gel and fluid lipid phases coexist, all of the probes partition into the fluid liquid-crystal phase to the same extent, regardless of the location of the fluorescent moiety, with the exception of the end-labeled 16-AP which also favors the fluid phase but much less strongly. In addition, all of the probes, including 16-AP, exhibit 5–7-fold greater partitioning out of Ca^{2+}-induced gel phase than thermotropic gel phases. We have previously reported a value of $R_{LC/G} = 18 \pm 2$ for the methyl ester of 12-AS in DOPS/(7,6)PC in excess Ca^{2+} [15]. Strong partitioning into the fluid phase has also been reported for 12-AS in DPPC/DLPC vesicles, utilizing measurements of fluorescence polarization [19].

It is reasonable that fatty acids with fluorescent labels attached at varying positions would disrupt lipid packing in the gel phase to varying degrees. An example of an effect of acyl chain perturbations on hydrocarbon chain packing is the classic study by Barton and Gunstone [20] on a series of 16-mono-unsaturated dioctadecenoylphosphatidylcholines, in which the lowest gel to liquid-crystal phase transition temperatures were observed for isomers with the *cis* double bond near the middle of the acyl chains. In the case of the *n*-(9-anthroyloxy) fatty acids, the fact that all of the probes partition out of thermotropic gel phases, and even more strongly out of the more rigid [15] $Ca(PS)_2$ gel phase, suggests that these probes also do not pack well into the gel lattice. The lack of a significant increase in probe fluorescence in the $Ca(PS)_2$ gel phase relative to fluid-phase DOPS is consistent with this conclusion. We have observed a 2-fold increase in fluorescence in $Ca(PS)_2$ over fluid DOPS for 1-acyl-2-[12-(9-anthroyloxy)stearoyl]phosphatidylserine, which partitions equally between Ca^{2+}-induced gel and fluid phases in DOPS/(7,6)PC multilayers [15].

The only positional dependence of probe partitioning that we observe is with 16-AP, where the fluorescent group is attached at the methyl terminal end of the acyl chain. Although the position of attachment at the chain terminus is the same for 16-AP as for 11-AU, this latter probe is much shorter in chain length than the surrounding lipid matrix. The short chain length of the 11-AU places the bulky (9-anthroyloxy) moiety in the midst of the lipid acyl chains. In contrast, with 16-AP the same bulky probe is positioned near the center of the lipid bilayer. Apparently, this position causes a smaller perturbation of lipid packing. As shown in Table I, 16-AP exhibits similar partition behavior to the rod-shaped DPH. In qualitative agreement with our findings, Cadenhead et al. [21] report DSC measurements at 20 mol% probe and fluorescence polarization measurements at 0.2 mol% probe that show the relative bilayer perturbation by three 9-anthroyloxy probes in DPPC multilayers to be 2-AP > 12-AS > 16-AP.

These findings have implications for the use of fluorescent probes to monitor such membrane phenomena as lateral diffusion, inter-bilayer lipid transfer, lipid phase separation, and membrane fusion. Our results demonstrate that the position of attachment of the fluorophore can influence how the probe distributes between gel and fluid lipid phases. Knowledge of such partition behavior is valuable in selecting a membrane probe. Of the *n*-(9-anthroyloxy) fatty acids, for example, 16-AP would be the most sensitive for monitoring lipid gel phases, and its phospholipid derivatives might prove to be even better probes. This study also demonstrates that homogeneous probe distribution in membrane lipid cannot be assumed, an important consideration in studies of heterogeneous membrane systems of complex lipid phase behavior.

References

1 Peters, R. and Beck, K. (1983) Proc. Natl. Acad. Sci. USA 80, 7183–7187.
2 McConnell, H.M., Tamm, L.K. and Weis, R.M. (1984) Proc. Natl. Acad. Sci. USA 81, 3249–3253.
3 Sklar, L.A., Miljanich, G.P. and Dratz, E.A. (1979) Biochemistry 18, 1707–1716.
4 Klausner, R.D. and Wolf, D.E. (1980) Biochemistry 19, 6199–6203.
5 Feigenson, G.W. (1983) Biochemistry 22, 3106–3112.
6 Parente, R.A. and Lentz, B.R. (1986) Biochemistry 25, 1021–1026.
7 Lenventis, R., Gagné, J., Fuller, N., Rand, R.P. and Silvius, J.R. (1986) Biochemistry 25, 6978–6987.
8 Klausner, R.D., Kleinfeld, A.M., Hoover, R.L. and Karnovsky, M.J. (1980) J. Biol. Chem. 255, 1286–1295.
9 Haverstick, D. and Glaser, M. (1987) Proc. Natl. Acad. Sci. USA 84, 4475–4479.
10 Thulborn, K.R. and Sawyer, W.H. (1978) Biochim. Biophys. Acta 511, 125–140.
11 Chalpin, D.B. and Kleinfeld, A.M. (1983) Biochim. Biophys. Acta 731, 465–474.
12 Chattopadhyay, A. and London, E. (1987) Biochemistry 26, 39–45.
13 London, E. and Feigenson, G.W. (1981) Biochemistry 20, 1932–1938.
14 London, E. and Feigenson, G.W. (1981) Biochim. Biophys. Acta 649, 89–97.
15 Florine, K.I. and Feigenson, G.W. (1987) Biochemistry 26, 1757–1768.
16 Caffrey, M. and Feigenson, G.W. (1981) Biochemistry 20, 1949–1961.
17 Mabrey, S. and Sturtevant, J.M. (1976) Proc. Natl. Acad. Sci. USA 73, 3862–3866.
18 Florine-Casteel, K. and Feigenson, G.W. (1988) Biochim. Biophys. Acta, submitted.
19 Bashford, C.L., Morgan, C.R. and Radda, G.K. (1986) Biochim. Biophys. Acta 426, 157–172.
20 Barton, P.G. and Gunstone, F.D. (1975) J. Biol. Chem. 250, 4470–4476.
21 Cadenhead, D.A., Kellner, B.M.J., Jacobson, K. and Papahadjopoulos, D. (1977) Biochemistry 16, 5386–5392.